Proceedings of the 5th World Congress on Mechanical, Chemical, and Material Engineering (MCM'19)
Lisbon, Portugal – August, 2019
Paper No. HTFF 172
DOI: 10.11159/htff19.172

The Formulation of the RANS Equations for Hypersonic Turbulent Flows

Haoyuan Zhang[1,2], Timothy Craft[1], Hector Iacovides[1]
[1] School of Mechanical, Aerospace and Civil Engineering, The University of Manchester
George Begg Building, Manchester M13 9PL, UK
[2] Computational Aerodynamics Institute, China Aerodynamic Research and Development Center
Mianyang, Sichuan, 621000, P. R. China
haoyuan.zhang@manchester.ac.uk; tim.craft@manchester.ac.uk
h.iacovides@manchester.ac.uk

Abstract **-** Accurate prediction of hypersonic turbulent flows is essential to the design of high-speed aerospace vehicles. Such flows are mainly predicted using the Reynolds-Averaged-Navier-Stokes (RANS) approach in general and in particular turbulence models using the effective viscosity approximation. Several terms involving the turbulent kinetic energy (TKE) appear explicitly in the RANS equations through the modelling of the Reynolds stresses and mean total energy and the molecular and turbulent diffusion terms. Some of these terms are often ignored in low, or even supersonic, speed simulations with zero-equation models, as well as some one- or two-equation models. The omission of these terms may not be suitable under hypersonic conditions, but there are nevertheless codes and software packages that still make such approximations, even for very high-speed turbulent flow simulations. To clarify the impact of ignoring the TKE terms in the RANS equations, two linear two-equation models and one nonlinear two-equation model are applied to the computation of two hypersonic benchmark cases, a 2D zero-pressure gradient flat plate case and an axisymmetric shock wave boundary layer interaction (SWBLI) case. The predicted surface friction coefficients and velocity profiles with different combinations of TKE terms showed little differences in the zero-pressure gradient case. However, in the SWBLI case, comparisons show that the flow separation would be delayed or accelerated with different combinations of TKE compared to the one with all the TKE terms included. Therefore, it is highly recommended to include all the TKE terms in the mean flow equations when dealing with simulations of hypersonic turbulent flows, especially for flows with shock wave boundary layer interactions. As a further consequence, since the TKE terms may not be obtained explicitly in zero-equation, or some one-equation, models, it is debatable whether these models are suitable for simulations of hypersonic turbulent flows with SWBLIs.

Keywords**:** Hypersonic flows; Turbulence modelling; SWBLIs; Turbulent kinetic energy

1. Introduction

The need for a reliable and cost-effective approach to travel through the atmosphere at hypersonic speed (Mach number > 5.0) has prompted a renewed interest in hypersonic flight vehicles. The design and optimisation of hypersonic vehicles, including accurate aerodynamic force prediction, requires a good understanding of complex hypersonic turbulent flows, which is one of the most important unsolved problems of classical physics. The development of modern computer technology provides an opportunity for solving turbulent flows problems using Computational Fluid Dynamics (CFD). The most practical approach for the simulations of many complex flows is via Reynolds-Averaged-Navier-Stokes (RANS) modelling for the consideration of cost and accuracy.

The classical Reynolds-Averaged Navier-Stokes (RANS) equations are based on incompressible flow assumptions, where the density is considered as constant. However, when the density variation is so significant that it cannot be ignored, the density should no longer be treated as constant. So, when dealing with compressible turbulent flows, not only the velocity and pressure fluctuations must be considered, but the density and temperature fluctuations must be accounted for as well. In such an approach the Favre, or mass, averaging is widely used to avoid the additional terms that would otherwise keep the mean conservation equations from having close analogues in the laminar equations.

When dealing with incompressible turbulent flow within the SIMPLE framework and using an eddy viscosity formulation to represent the turbulent stresses, a term of $\frac{2}{3}\overline{\rho}k$ ($\overline{\rho}$:mean density, k:turbulent kinetic energy) that arises from

the eddy viscosity model (EVM), which could be combined with the pressure in the mean momentum equation, is often ignored. For the low speed or supersonic compressible turbulent flows, the omission of the above term, as well as the TKE terms in the mean energy equations, often take place. This approach may not be suitable under hypersonic conditions, but nevertheless such approximations, even for very high-speed turbulent flow simulations, are often made. Rumsey [1] validated compressibility corrections of the *k-ω* models by examining hypersonic zero-pressure gradient boundary layer flows using the CFL3D [2] code, in which the TKE terms in both the mean momentum and energy equations are not included. The resulting comparisons showed that little difference was seen when comparing the computations of the CFL3D and VULCAN [3] codes, the latter of which includes all TKE terms. However, Wilcox [4] pointed out that "at hypersonic speeds ρk may be a significant fraction of p", which means that the TKE should not be ignored in the momentum equation. Since different authors treated the TKE terms in different ways, sometimes it is difficult to obtain a uniform evaluation from different papers for the same turbulence models on the performance of hypersonic turbulent flow predictions.

In this paper, to investigate the impact of ignoring the TKE terms in the RANS equations, a new density based solver was developed within OpenFOAM (Open source Field Operation and Manipulation), based on the AUSMPW$^+$ convection scheme [5], that contains different ways of including, or not including, the relevant TKE terms in the mean momentum and energy equations. Two linear eddy-viscosity models, namely the two-equation *k-ε* model of Launder and Sharma [6] with the Yap correction [7] (LSY model) and the two-equation *k-ω* model of Menter [8] (SST model), and one nonlinear eddy-viscosity model, the two-equation *k-ε* model of Craft et al. [9] (CLS model), are applied to the computations of two hypersonic benchmark cases, a 2D zero-pressure gradient flat plate case and an axisymmetric shock wave boundary layer interaction (SWBLI) case. The open source CFD code OpenFOAM V4.1 is used to implement the new density-based compressible solver and the nonlinear turbulence model.

2. Physical Model

Under the continuum mechanics assumption, the Favre-averaged Navier–Stokes equations are often used for describing the unsteady turbulent flows of compressible viscous fluids. Besides the transport equations for the mean variables, additional equations, such as those for the Reynolds stresses, the turbulent variables, and other state and heat transfer correlations, are required to close the whole partial differential equation (PDE) system.

2.1. Governing Equations

For an unsteady compressible flow, the transport equations for mean mass, momentum and energy may be written as:

$$\frac{\partial \overline{\rho}}{\partial t} + \frac{\partial}{\partial x_i}(\overline{\rho}\tilde{u}_i) = 0 \tag{1}$$

$$\frac{\partial}{\partial t}(\overline{\rho}\tilde{u}_i) + \frac{\partial}{\partial x_j}\left(\overline{\rho}\tilde{u}_j\tilde{u}_i\right) = -\frac{\partial \overline{p}}{\partial x_i} + \frac{\partial}{\partial x_j}\left(\tilde{\sigma}_{ij} - \overline{\rho u_j'' u_i''}\right) \tag{2}$$

$$\frac{\partial}{\partial t}[\overline{\rho}\tilde{E}] + \frac{\partial}{\partial x_j}\left[\overline{\rho}\tilde{u}_j\left(\tilde{E} + \overline{p}\right)\right] = \frac{\partial}{\partial x_j}\left[\tilde{u}_i\left(\tilde{\sigma}_{ij} - \overline{\rho u_j'' u_i''}\right)\right] - \frac{\partial}{\partial x_j}\tilde{q}_j + \frac{\partial}{\partial x_j}\left[-c_p\overline{\rho u_j'' T''} + \overline{u_i''\sigma_{ij}} - \overline{\rho u_j'' \tfrac{1}{2} u_i'' u_i''}\right] \tag{3}$$

where $\overline{\rho}$, $\tilde{u}_i$, $\overline{p}$ and $\tilde{E}$ are the mean density, velocity, pressure and total energy with $\overline{}$ representing time-averaged values and $\tilde{}$ representing mass-averaged values. Obeying the perfect gas assumption, the equation of state and the total energy are

$$\bar{p} = (\gamma - 1)\overline{\rho}\tilde{e}, \qquad \tilde{E} = \tilde{e} + \tfrac{1}{2}\tilde{u}_i\tilde{u}_i + k \tag{4}$$

where $\tilde{e} = c_v T$ is the specific internal energy and k is the turbulent kinetic energy. $\gamma = \frac{c_p}{c_v}$ is the ratio of specific heats and c_p and c_v are the specific heats at constant pressure and volume respectively. The terms $\tilde{\sigma}_{ij} - \overline{\rho u_j'' u_i''}$ is the mean total stress tensor, which includes both the molecular and turbulent parts. For a Newtonian fluid, the mean molecular viscous stress is $\tilde{\sigma}_{ij} = \mu\left(\frac{\partial \tilde{u}_i}{\partial x_j} + \frac{\partial \tilde{u}_j}{\partial x_i} - \frac{2}{3}\frac{\partial \tilde{u}_k}{\partial x_k}\delta_{ij}\right)$, in which the dynamic viscosity μ is determined by Sutherland's law. Similarly, $\tilde{q}_j$, the molecular heat flux, can be written as $\tilde{q}_j = -\gamma \frac{\mu}{Pr} c_v \frac{\partial T}{\partial x_j}$ with Prandtl number Pr = 0.72 for the air flows considered here.

The turbulent Reynolds stress $\tilde{\tau}_{ij} = -\overline{\rho u_j'' u_i''}$ and turbulent heat flux $\tilde{q}_{T,j} = c_p \overline{\rho u_j'' T''}$ and the so-called molecular diffusion term of $\overline{u_i'' \sigma_{ij}}$ and turbulent transport term of $\overline{\rho u_j'' \frac{1}{2} u_i'' u_i''}$ are need to be modelled in order to close this whole PDE system.

2.2. Turbulence modelling

The turbulence models used in this paper are all EVMs, so the Reynolds stress can be modelled with the general form (up to cubic terms) of the following expression

$$\begin{aligned} -\overline{\rho u_i'' u_j''} = & -\frac{2}{3}\bar{\rho} k \delta_{ij} + \mu_t S_{ij} \\ & - \left[C_1 \frac{\mu_t}{\tilde{\varepsilon}}\left(S_{ik}S_{jk} - \frac{1}{3}S_{mk}S_{mk}\delta_{ij}\right) + C_2 \frac{\mu_t}{\tilde{\varepsilon}}\left(\Omega_{ik}S_{kj} + \Omega_{jk}S_{ki}\right) + C_3 \frac{\mu_t}{\tilde{\varepsilon}}\left(\Omega_{ik}\Omega_{jk} - \frac{1}{3}\Omega_{lk}\Omega_{lk}\delta_{ij}\right) \right. \\ & + C_4 \frac{\mu_t k}{\tilde{\varepsilon}^2}\left(\Omega_{ki}S_{lj} + S_{kj}\Omega_{li}\right)S_{kl} + C_5 \frac{\mu_t k}{\tilde{\varepsilon}^2}\left(\Omega_{il}\Omega_{lm}S_{mj} + S_{il}\Omega_{lm}\Omega_{mj} - \frac{2}{3}S_{lm}\Omega_{mn}\Omega_{nl}\delta_{ij}\right) \\ & \left. + C_6 \frac{\mu_t k}{\tilde{\varepsilon}^2} S_{ij}S_{kl}S_{kl} + C_7 \frac{\mu_t k}{\tilde{\varepsilon}^2} S_{ij}\Omega_{kl}\Omega_{kl} \right] \end{aligned} \tag{5}$$

where $S_{ij} = \left(\frac{\partial \tilde{u}_i}{\partial x_j} + \frac{\partial \tilde{u}_j}{\partial x_i}\right) - \frac{2}{3}\frac{\partial \tilde{u}_k}{\partial x_k}\delta_{ij}$ and $\Omega_{ij} = \left(\frac{\partial \tilde{u}_i}{\partial x_j} - \frac{\partial \tilde{u}_j}{\partial x_i}\right)$ are the strain rate and vorticity, respectively and μ_t is the turbulent eddy viscosity. If $C_1 \sim C_7$ all equal zero, this form is the so-called Boussinesq approximation and the model under this approximation is often also called a linear EVM. Otherwise, models making use of some, or all, of the non-linear terms in the above stress-strain relation can be referred to as non-linear EVMs. In this paper, all the turbulence models used are in their original forms, so the details of each model can be found in references [6]-[9].

The turbulent heat fluxes $\tilde{q}_{T,j} = c_p \overline{\rho u_j'' T''}$ are modelled using the simple eddy-diffusivity approximation which can be written as $\tilde{q}_{T,j} = c_p \overline{\rho u_j'' T''} = -\frac{\mu_t c_p}{Pr_t}\frac{\partial \tilde{T}}{\partial x_j}$ with turbulent Prandtl number Pr_t = 0.9. An approximation of a gradient expression for the molecular diffusion and turbulent transport appearing in the mean energy equation is used here as follows:

$$\overline{\sigma_{ij} u_j''} - \overline{\rho u_j'' \frac{1}{2} u_i'' u_i''} = \left(\mu + \frac{\mu_t}{\sigma_k}\right)\frac{\partial k}{\partial x} \tag{6}$$

where σ_k is a model coefficient.

2.3. Presence of the Turbulent Kinetic Energy

Following the eddy viscosity assumption, the transport equations (2) and (3), under the Boussinesq approximation for the turbulent stresses, can be rewritten as

$$\frac{\partial}{\partial t}(\overline{\rho}\tilde{u}_i) + \frac{\partial}{\partial x_j}(\overline{\rho}\tilde{u}_j\tilde{u}_i) = -\frac{\partial \overline{p}}{\partial x_i} + \frac{\partial}{\partial x_j}\left[\underbrace{(\mu+\mu_t)\left(\frac{\partial \tilde{u}_i}{\partial x_j} + \frac{\partial \tilde{u}_j}{\partial x_i} - \frac{2}{3}\frac{\partial \tilde{u}_k}{\partial x_k}\delta_{ij}\right)}_{(d)} - \underbrace{\frac{2}{3}\overline{\rho}k\delta_{ij}}_{(a)}\right] \tag{7}$$

$$\begin{aligned}\frac{\partial}{\partial t}\left[\overline{\rho}\left(\tilde{e} + \tfrac{1}{2}\tilde{u}_i\tilde{u}_i + \underbrace{k}_{(b)}\right)\right] + \frac{\partial}{\partial x_j}\left[\overline{\rho}\tilde{u}_j\left(\left(\tilde{e} + \tfrac{1}{2}\tilde{u}_i\tilde{u}_i + \underbrace{k}_{(b)}\right) + \overline{p}\right)\right] \\ = \frac{\partial}{\partial x_j}\left[\tilde{u}_i\left[\underbrace{(\mu+\mu_t)\left(\frac{\partial \tilde{u}_i}{\partial x_j} + \frac{\partial \tilde{u}_j}{\partial x_i} - \frac{2}{3}\frac{\partial \tilde{u}_k}{\partial x_k}\delta_{ij}\right)}_{(d)} - \underbrace{\frac{2}{3}\overline{\rho}k\delta_{ij}}_{(a)}\right]\right] - \frac{\partial}{\partial x_j}\left(\frac{\mu}{Pr} + \frac{\mu_t}{Pr_t}\right)c_p\frac{\partial T}{\partial x_j} + \underbrace{\left(\mu + \frac{\mu_t}{\sigma_k}\right)\frac{\partial k}{\partial x}}_{(c)}\end{aligned} \tag{8}$$

For the nonlinear EVM, the two equations above retain the same form, except for the term (*d*), which should then contain contributions from the non-linear terms as well. In the Eqns. (7) and (8), there are three different terms related to TKE which are often neglected. The term (*a*) in Eqn. (7) is often ignored, or absorbed into the pressure term when dealing with incompressible turbulence flows. The terms (*b*) and (*c*) in Eqn. (8) are also often ignored for high speed compressible turbulent flows. Table 1 lists three possible combinations for the presence or absence of these terms which have been found in software, or reported in research papers. For combination "C1", all three terms are ignored, which is commonly used for incompressible simulations. In OpenFOAM V4.1, the integrated density based compressible solver rhoCentralFoam also takes this approach. The second combination, "C2", includes the TKE term of (*a*) but neglects terms (*b*) and (*c*), which is often a reasonable approximation since $k \ll \tilde{E}$ in most flows of engineering interest. The last combination "C3" includes all the TKE terms.

Table 1: Three combinations of TKE terms in RANS equations.

Combinations	Term (*a*)	Term (*b*)	Term (*c*)
C1	Not included	Not included	Not included
C2	Included	Not included	Not included
C3	Included	Included	Included

3. Numerical Implementation

The conservation equation for a general variable scalar $\phi = \phi(\boldsymbol{x}, t)$ can be expressed as

$$\frac{\partial \phi}{\partial \mathrm{t}} + \nabla \cdot (\mathbf{u}\phi) - \nabla \cdot \left(\Gamma_\phi \nabla \phi\right) = S_\phi(\phi) \tag{9}$$

where $\frac{\partial \phi}{\partial \mathrm{t}}$ is the transient term, $\nabla \cdot (\mathbf{u}\phi)$ is the convection term, $\nabla \cdot \left(\Gamma_\phi \nabla \phi\right)$ is the diffusion term, $S_\phi(\phi)$ is the source term, Γ_ϕ is the diffusivity. This whole PDEs system is solved with Finite Volume Methods (FVM) on any three-dimensional unstructured grid of polygonal cells via OpenFOAM, which is an open source software for computational fluid dynamics (CFD). For the present study, the software package of OpenFOAM V4.1 is employed, which includes a variety of density-based and pressure-based solvers for compressible flows. As this research is mainly concerned with the hypersonic flow, based on the density-based compressible solver, rhoCentralFoam, a new solver with the three different optional TKE terms in Table 1 has been implemented. In high speed flows the representation of the convection terms is crucial for accuracy. In this study the AUSMPW$^+$ scheme is used to calculate the convection term for all the variables. To keep the solution bounded and achieve high resolution around shocks, the Total Variation Diminishing (TVD) interpolation with the van-Albada limiter is used for the interface calculations.

Like the new density solver, the CLS non-linear turbulence model has also been implemented into OpenFOAM, in a similar way to how the Launder-Sharma k-ε model is coded. The major difference between the two is the use of the non-linear constitutive relation of Eqn. (5) in the former, using the model coefficients from [9].

4. Results

4.1. 2D zero-pressure gradient flat plate

The 2-D zero-pressure gradient flat plate is a fundamental benchmark case which is widely used for the verification and validation of RANS models as well as numerical solvers on compressible turbulent boundary layer predictions. The data used for comparison here are obtained directly from the online database named "Turbulence Modelling Resource" hosted by the Langley Research Centre. The boundary conditions are given in Table 3 and the working medium is dry air, which can be treated as a thermally and calorically perfect gas since the total temperature is 1800 K. A mesh of 128×128 is used to run all the simulations in this section. The distance of the first cell off the wall is set to be $2.0 \times 10^{-6} m$ which maintains the y^+ at the wall for all the simulations to be less than 1.0.

Table 2: Boundary conditions of the 2D zero-pressure gradient boundary layer.

M_∞	Re_∞/m	T_∞	T_w	T_o
5	15,000,000	300K	817.5K	1800K

In Figure 3, the wall skin friction predicted by LSY model, SST model and CLS model, at Re_θ, the Reynolds number based on momentum thickness, between 4000 and 12000, are compared. The velocity profiles, at Re_θ of 10000, are compared in Figure 4. Firstly, the predicted C_f, wall friction coefficient, and velocity profiles matching the theoretical results within a reasonable error tolerance for all three turbulence models shows that the new density-based compressible solver and the non-linear CLS model are implemented properly within the OpenFOAM V4.1 framework. Secondly, for all models, the predicted C_f values show very little difference and the velocity profiles predicted by each model are practically identical.

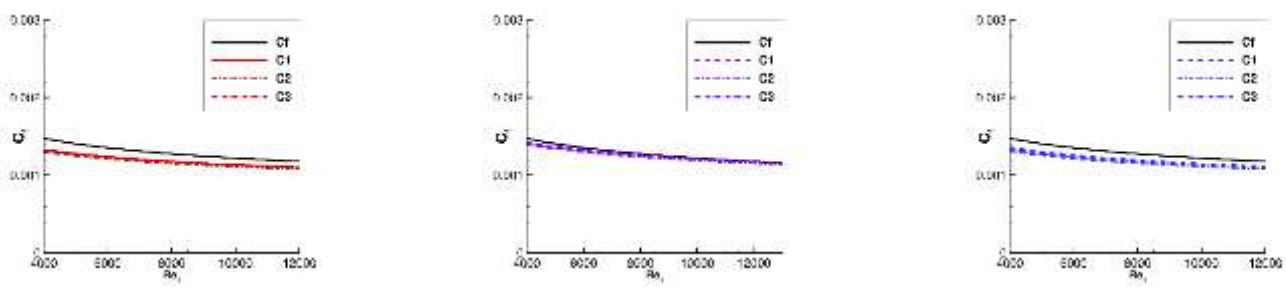

Fig. 1: Comparison of wall skin friction of LSY (left), SST (middle) and CLS (right) models.

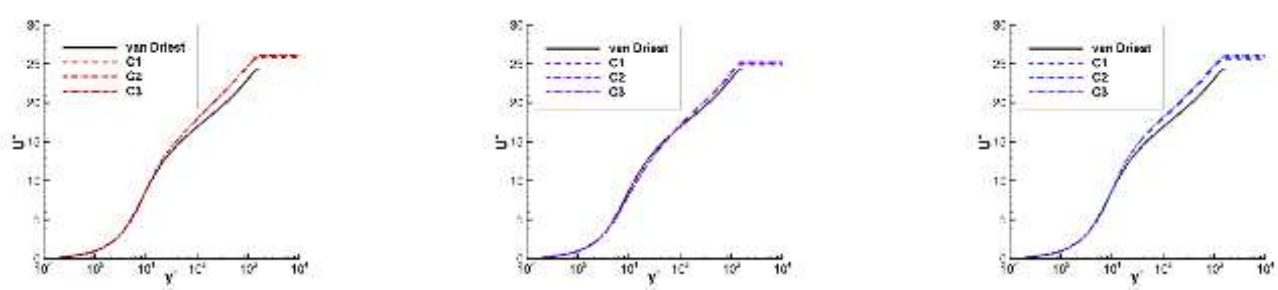

Fig. 2: Comparison of velocity profiles at Re_θ=10000 of LSY (left), SST (middle) and CLS (right) models.

The results above indicate that including or neglecting the TKE terms of (*a*), (*b*) or (*c*) has only a limited effect only the solution of the RANS equations in this case, implying that the assumptions of $\bar{\rho}k \ll \bar{p}$ and $k \ll \tilde{E}$ do hold in the hypersonic zero-pressure gradient boundary layer flow. To check this, the ratios of $\frac{2}{3}\bar{\rho}k/\bar{p}$ and $k/\tilde{E}$ predicted by the LSY and the CLS model, at Re_θ of 10000, are presented in Figure 5. The ratio of $\frac{2}{3}\bar{\rho}k/\bar{p}$ is less than 5% and the ratio of $k/\tilde{E}$ is even smaller, with a maximum value of less than 2%, for both models. So, for the simple zero-pressure gradient boundary layer flows, the introduction of the TKE terms results in little difference and does not affect the validation of the performance of turbulence models.

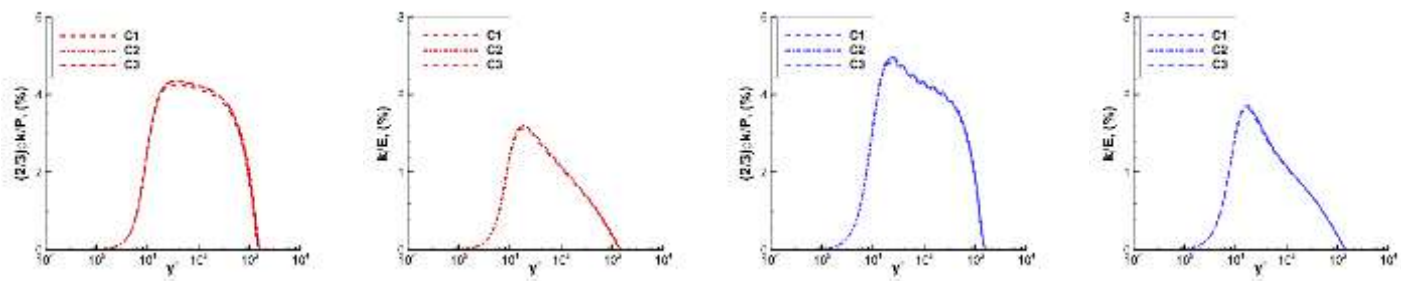

Fig. 3: Comparison of the ratios of $\frac{2}{3}\bar{\rho}k/\bar{p}$ and $k/\tilde{E}$ predicted by the LSY (left two) and CLS (right two) model at Re_θ=10000.

4.2. Axisymmetric Compression Corner

The axisymmetric compression corner is a benchmark case which is widely used and accepted to test the ability of turbulence models to predict a hypersonic flow field with shock wave induced separation. The experiments of Kussoy and Horstman [10] at Mach number 7.05 serve as the test case for the validation of different turbulence models. All the experimental data used in this chapter are obtained from the comprehensive review of the hypersonic shock wave boundary layer interaction database of Settles and Dodson [11].

The test model of the experiments is shown in Figure 6, for which a flare angle θ of 35° is considered in this section. The nominal freestream conditions are given in Table 4. Since the total temperature of the experiments was around 900 K, the working medium, dry air, is assumed to be a thermally and calorically perfect gas. The inlet boundary condition was obtained by calculating a cylinder boundary layer flow and matching the measured and computed displacement thickness at 6 cm ahead of the corner.

Table 3: Freestream conditions of the axisymmetric compression corner case.

M_∞	Re_∞/m	T_∞, K	T_w, K	$p_\infty, N/m^2$	T_{total}, K
7.05	58,000,000	81.2	311	576	888.37

The computations are performed using a 200×200 structured grid, uniform in the streamwise direction and expanding exponentially in the wall normal direction. The y^+ at the first grid point off the wall is kept at a value of less than 0.3. The lengths of cylinder and flare are both set to be 20 centimetres, which are long enough to cover the whole interaction region. The whole computational domain and the grid of 35° flare are shown in Figure 7.

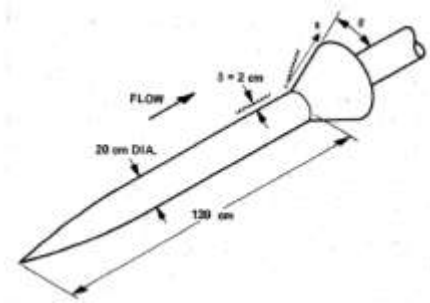

Fig. 4: The test model of Kussoy and Horstman experiment.

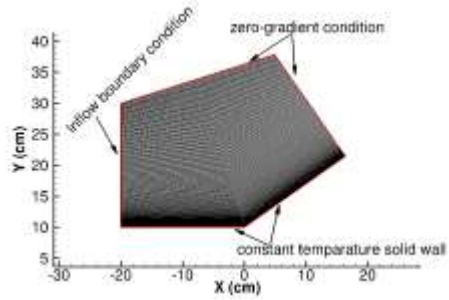

Fig. 5: Grid for axisymmetric compression corner.

The predicted surface pressure and wall heat transfer rate with the various TKE terms included, or excluded, from all three models are compared in Figures 8 and 9. Unlike the first case, significant differences now exist between the three treatments of TKE, the most significant of which is the size of the separation region. The three turbulence models show similar variation patterns. The C1 combination returns the smallest separation bubble. In contrast, the C2 combination of terms results in the largest separation, and the C3 results are somewhere in between. The peak value of the surface pressure shows a smaller variation between results than the peak value of the wall heat transfer rate. With all the TKE terms of (a), (b) and (c) included, the nonlinear CLS model agrees best with the measured pressure profiles, which suggests that the nonlinear CLS model has a better capability of separation prediction than the linear models. The LSY model tends to under-estimate the separation and the SST model, by contrast, tends to over-estimate the separation. All of the models return much higher wall heat flux peak values than the experimental data in the interaction region.

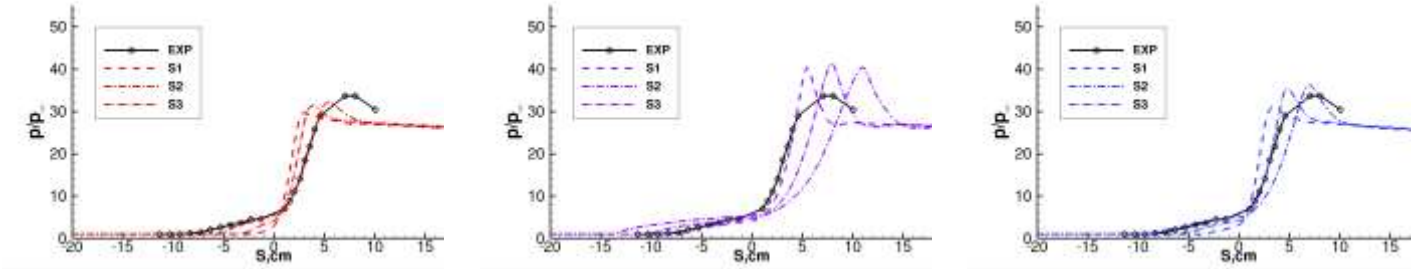

Fig. 6: Comparison of wall pressure of LSY (left), SST (middle) and CLS (right) models.

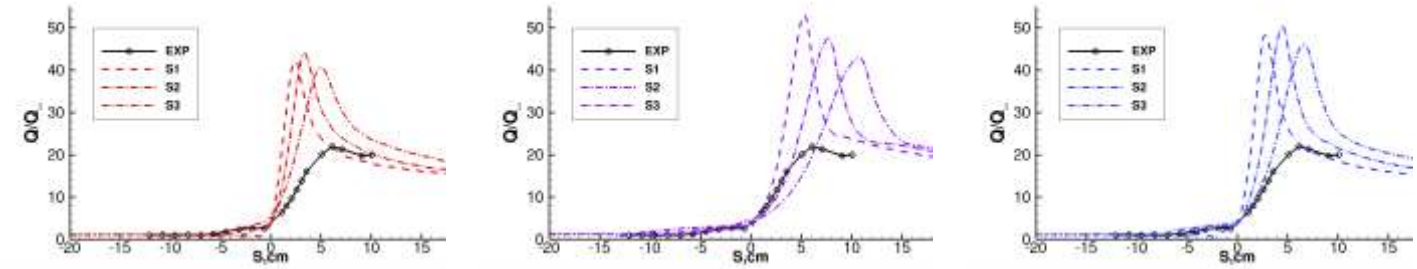

Fig. 7: Comparison of wall heat transfer rate of LSY (left), SST (middle) and CLS (right) models.

The significant differences in flow separation around the interaction corner indicate that the ratios of $\frac{2}{3}\bar{\rho}k/\bar{p}$ and $k/\tilde{E}$ in this region must be quite different from the 2D zero-pressure gradient flat plate case. The comparison of these ratio for the CLS model around the corner, for the three treatments of TKE, is shown in Figures 10 and 11. Around the interaction

zone, the peak value of the ratio of $\frac{2}{3}\overline{\rho}k/\bar{p}$ reaches at least 40% for all three combinations, which indicates that ignoring the term of $\frac{2}{3}\overline{\rho}k$ would have a strong influence on the balance of terms in the mean momentum equation. The most significant effect of this influence is the pressure distribution in the interaction region, which has a strong impact on the flow separation and reattachment. The peak value of the ratio of $k/\tilde{E}$ is more than 12%, which affects the conservation of the mean velocity and static temperature. As the pressure is solved by the equation of state for compressible flow, this will also have some influence on the pressure distribution.

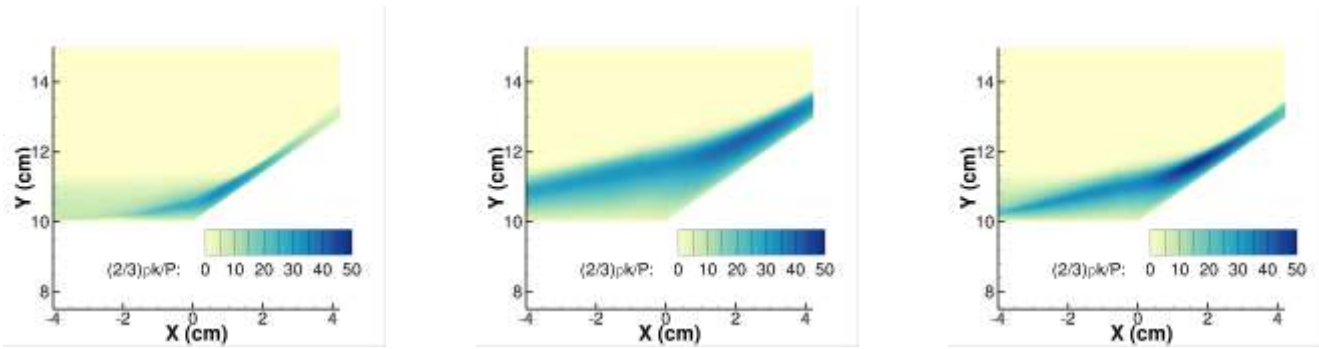

Fig. 8: Comparison for the ratio of $\frac{2}{3}\overline{\rho}k/\bar{p}$ of the CLS model at C1 (left), C2 (middle) and C3(right) combinations.

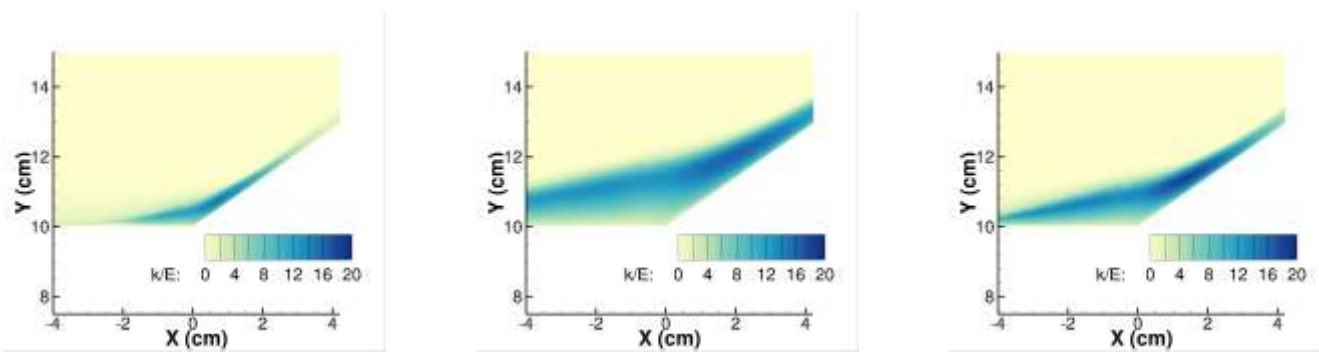

Fig. 9: Comparison for the ratio of $k/\tilde{E}$ of the CLS model at C1 (left), C2 (middle) and C3(right) combinations

These comparisons between these three treatments of TKE suggest that the assumptions of $\overline{\rho}k \ll \bar{p}$ and $k \ll \tilde{E}$ no longer hold in the interaction region of the hypersonic flows involving shock wave boundary layer interactions, especially with flow separation. The TKE terms of (*a*), (*b*) and (*c*) should therefore not be neglected when computing such flows.

5. Conclusion

The role of some terms involving TKE that are often neglected from the compressible RANS equations has been investigated by examining two typical hypersonic benchmark cases. Three different combinations of including, or neglecting, these terms included in the mean momentum and energy equations have been compared.

In simple zero-pressure gradient boundary layer flow, the numerical results showed that ignoring the three terms that are often neglected in incompressible, as well as some high-speed, cases had only limited impact on the flow field and surface variables. However, in the hypersonic flows with SWBLI, the TKE terms played a very important role in the conservation of mean momentum and energy equations. Compared to including all the TKE terms in the RANS equations, ignoring all of them could delay the flow separation. In contrast, neglecting only the terms in the mean total energy definition and the molecular diffusion and turbulent transport could accelerate the separation significantly.

In general, with all the TKE terms included, the nonlinear CLS model returned a more accurate flow structure than the linear model in terms of flow separation and surface pressure distribution, but all models failed to predict accurately the experimental variation of the wall heat flux, suggesting some further model refinement is necessary in the shock wave boundary layer interaction region.

From the above findings, it is recommended that all these three terms should be included when running hypersonic turbulent flow simulations. As a consequence, the use of very simple turbulence models that do not provide TKE explicitly, and are therefore unable to represent these terms when simulating hypersonic turbulent flows with SWBLIs, is debatable.

References

[1] C. L. Rumsey, "Compressibility Considerations for kw Turbulence Models in Hypersonic Boundary-Layer Applications," *Journal of Spacecraft and Rockets,* vol. 47, no. 1, pp. 11-20, 2010.

[2] S. L. Krist, R. T. Biedron, and C. L. Rumsey, "CFL3D user's manual (version 5.0)," 1998.

[3] J. White and J. Morrison, "A pseudo-temporal multi-grid relaxation scheme for solving the parabolized Navier-Stokes equations," in *14th Computational Fluid Dynamics Conference*, 1999, p. 3360.

[4] D. C. Wilcox, *Turbulence Modeling for CFD,* 3rd ed. La Canada, CA: DCW Industries, 2006.

[5] K. H. Kim, C. Kim, and O. H. Rho, "Methods for the accurate computations of hypersonic flows - I. AUSMPW+ scheme," (in English), *Journal of Computational Physics,* vol. 174, no. 1, pp. 38-80, Nov 20 2001.

[6] B. E. Launder and B. I. Sharma, "Application of the energy-dissipation model of turbulence to the calculation of flow near a spinning disc," *Letters in Heat and Mass Transfer,* vol. 1, pp. 131-138, 1974.

[7] C. R. Yap, "Turbulent heat and momentum transfer in recirculating and impinging flows," Ph.D Thesis, Faculty of Technology, University of Manchester, 1987.

[8] F. R. Menter, M. Kuntz, and R. Langtry, "Ten years of industrial experience with the SST turbulence model," *Turbulence, heat and mass transfer,* vol. 4, no. 1, pp. 625-632, 2003.

[9] T. J. Craft, H. Iacovides, and J. H. Yoon, "Progress in the use of non-linear two-equation models in the computation of convective heat-transfer in impinging and separated flows,", *Flow Turbulence and Combustion,* vol. 63, no. 1-4, pp. 59-80, 2000.

[10] M. I. Kussoy and C. C. Horstman, "Documentation of two- and three dimensional hypersonic shock wave/turbulent boundary layer interaction flows.," in "NASA Technical Memorandum," 1989.

[11] G. S. Settles and L. J. Dodson, "Hypersonic shock/boundary-layer interaction database: new and corrected data," *Pennsylvania State Univ. Report,* 1994.